Scientific Visualization, 2025, volume 17, number 2, pages 44 - 56, DOI: 10.26583/sv.17.2.04

Two-Channel High-Temperature Combustion Imaging System Based on High-Speed Cameras EVERCAM F 1000-16-C

F.A. Gubarev[1], L.Yu. Davydova[2], M.S. Tsiron[3]

Sevastopol State University (SevSU)

[1] ORCID: 0000-0002-7499-6109, gubarevfa@mail.ru
[2] ORCID: 0009-0003-7026-9670, lydavydova@sevsu.ru
[3] ORCID: 0009-0006-6687-4319, rwtciron@mail.ru

Abstract

The paper presents the results of using Evercam F 1000-16-C high-speed cameras for high-speed visualization of laser initiation and high-temperature combustion of Al-CuO thermite mixture. The possibility of determining process parameters based on the results of high-speed shooting is demonstrated. Two visualization modes are considered: synchronous operation of two cameras to obtain images from two angles, and synchronous operation of two cameras as part of a laser monitor with a copper bromide vapor brightness amplifier. In the case of direct video recording, one of the cameras acts as the master one, and the recording frequency is set in the service program. It is proposed to use a two-angle video recording mode to study the spread of flame in a volume. For the first time, Evercam F 1000-16-C cameras were used as part of a laser monitor with a copper bromide vapor brightness amplifier. Laser monitoring, combined with direct video recording, makes it possible to study the surface of a sample in the area of igniting laser interaction and flame propagation in one of the planes. A feature of the operation of Evercam cameras as part of a laser monitor is the need to generate trains of clock pulses synchronized with the radiation pulses of the brightness amplifier and the radiation pulse of the igniting laser. In this case, both cameras work in slave mode. The synchronization unit is designed using the STM32F103C8T6 microcontroller board and has galvanically isolated input and output signals.

Keywords: high-speed visualization, Evercam, synchronization, laser monitor, brightness amplifier, high-temperature combustion.

1. Introduction

Currently, the issues of high-speed visualization of processes are relevant for solving many research tasks [1-12]. This is due to the possibility of a detailed study of the dynamics of processes over time in order to discover new phenomena and effects, determine the patterns of development and flow of physical and chemical processes. High-speed cameras of both foreign and Russian production are often used as image acquisition tools, while the research methodology and experimental schemes may differ depending on the characteristics of the environment and the dynamics of the processes.

The most common high-speed cameras for scientific imaging can be highlighted based on the experience of implementing research projects in various fields [13]. In [1], a Photron Fastcam SA5 high-speed camera (USA) was used to record the gas-dynamic shock-wave flow. In [2], the splash generation process was recorded by a NAC Memrecam HX-3 high-speed camera (Japan). The course of plasma-chemical processes in [3] was monitored using an industrial camera Baumer VLG-20 (Switzerland) and a high-speed monochrome camera Fastec Imaging IN250M512 (USA). In work [4], an Evercam 1000-4-C high-speed camera (Russia) was used to visualize the process of electrode metal transfer. When conducting experimental

research in the field of military weapons and military equipment [5], high-speed photography was carried out with an Evercam 4000-8-M camera (Russia). The combustion of high-energy materials was studied using cameras Fastec Imaging HiScpec1 [14], Vision Research Phantom v2512 [15], Vision Research Phantom Miro M110 [6, 10], NAC Memrecam HX-6 [13], Photron Fastcam SA1 [7].

The difficulty of studying the combustion of high-energy materials and high-temperature processes in general is not only the high speed of the processes, but also the high brightness of the radiation accompanying the process [12]. To study such materials or processes, equipment is required to reduce the influence of bright background lighting. The main technical solutions involve the use of systems with active filtration and laser illumination [15]. These systems require synchronization of frame recording and backlighting. This principle of visualization is implemented in works [14, 15].

In some visualization tasks, it is necessary to synchronize two high-speed cameras [8, 16] to obtain two sequences of frames in order to increase the information content of the visualization process. As a rule, the camera manufacturer provides an option for connecting cameras in a “master-slave” mode [17, 18]. The master camera generates electric pulses synchronous with the exposure, which are fed to the sync input of the slave camera.

When studying the processes of laser initiation of combustion, synchronization of the laser pulse with the beginning of recording is required [7, 9, 11].

The most technically difficult options for visualizing combustion processes are systems using a single- or two-channel laser monitor based on a pulse-periodic brightness amplifier containing two high-speed cameras and a single-pulse laser that initiates combustion [19, 20]. Laser monitor with a copper bromide active medium is a domestic development that makes it possible to visualize the surface of burning materials through the bright glow created by the flame. The laser monitor based on an active medium in copper bromide vapor has a high spectral brightness and a short radiation pulse duration (20-40 ns) [21, 22].

Currently, systems similar to [19, 20] are implemented based on high-speed cameras of the Phantom and Photron brands. In recent years, Russian-made Evercam cameras have become an alternative to foreign analogues [23]. Their operation has a number of features compared to common models; in particular, the synchronization principle is different, which is of fundamental importance when working as part of a laser imaging system with pulsed brightness amplifier. Therefore, the aim of this work is the practical implementation of various synchronization modes of Evercam 1000-4-C cameras and the design of an experimental setup for studying the process of laser initiation of high-energy materials using these cameras.

2. Experimental technique

2.1 Visualization object

The visualization object was a thermite mixture of Al-CuO prepared from aluminum and copper oxide nanopowders obtained by electric explosion of a wire [24]. The particle size distribution was close to normal logarithmic with a maximum of 90 nm for aluminum nanopowder and 50 nm for copper oxide nanopowder. To prepare the thermite mixture, two-stage mixing was used. Nanopowders were poured into a small-volume container with a weight ratio of aluminum and copper oxide powders of 1:4 with the addition of isopropyl alcohol. Initially, mixing was carried out in a “drunk barrel” type mixer (TUBULA S 2.0). For finer homogenization of the mixture, ultrasonic mixing was used [25]. An ultrasonic disperser was used with an emitter power of 75 W, a frequency of 22 kHz for 10 minutes. Next, the powders were placed in a drying oven to evaporate the alcohol.

The samples, made in the form of a rectangular parallelepiped with a size of 20×3×3 mm, had a weight of 150 mg and were placed on an aluminum substrate with a thickness of 2 mm. For initiation, a diode laser RLS-6-638/5-SMA-TEC (Russia) with a wavelength of 638 nm with a fiber optic output was used. The radiation from the initiating laser was directed to the

front surface of the sample, which was placed at the focus of the laser beam. The laser power in continuous mode could vary in the range from 0.2 to 2 W. Taking into account losses in the optical fiber and at the focusing system, the radiation power measured at the sample site in continuous mode could vary from 0.15 to 1.5 W. The diameter of the spot on the object was 0.6 mm, which provided a maximum power density of 5.3 W/mm^2. The laser had an external modulation input, which made it possible to set the duration of the laser pulse and, accordingly, the energy of the laser impact. At maximum laser power, initiation occurred at a pulse duration of 50 ms.

2.2 Two-angle direct visualization scheme

Fig. 1a depicts a two-angle visualization scheme based on two Evercam 1000-16-C high-speed cameras (Russia). The cameras are located at an angle of 90^0 to each other and record frontal (camera 1) and lateral (camera 2) images of the object of study in the sample's own glow. A Canon Macro Lens EF 100 mm lens is installed on the front camera, and an MC Zenitar 1.2/50s lens is installed on the side camera. The front camera has a field of view of 46 mm in width, the side one – 73 mm. Since the combustion of the Al-CuO thermite mixture is accompanied by a bright glow and scattering of combustion products, gray filters of the NS type are installed in front of the camera lenses to reduce illumination [26]. To prevent damage to the optical elements, protective quartz glass is installed in front of the gray filters and the initiating laser lens.

Images were recorded with a speed of 5000 frames/s. The spatial resolution of the matrix was set to 640×192 pixels. A special feature of the Evercam 1000-16-C is the ability to work with a full horizontal matrix resolution of 1920 pixels. As the shooting speed increases, the vertical resolution decreases.

The cameras were synchronized according to the scheme recommended by the manufacturer [23], in which camera 1 acted as the master and camera 2 as the slave. The corresponding connection of camera connectors is shown in Fig. 1b. Recording by the master camera begins at the leading edge of the signal at the "EXT REC IN" input and continues until the number of recorded pulses reaches a preset software value or a value limited by the capacity of the built-in memory. In this case, the duration of the signal at the "EXT REC IN" input does not affect the recording, but should not exceed the duration of the entire recording $t_p=N_p/f$, where N_p is the preset number of recorded images, f is the recording speed (frames per second). This feature of the camera operation allows the same signal to be supplied to the "EXT REC IN" input of the camera and to the laser enable input, which generates the duration of the laser radiation in accordance with the pulse duration of the enable pulse. To generate laser pulses with a duration of up to 400 ms, a single-channel UTG962E was used.

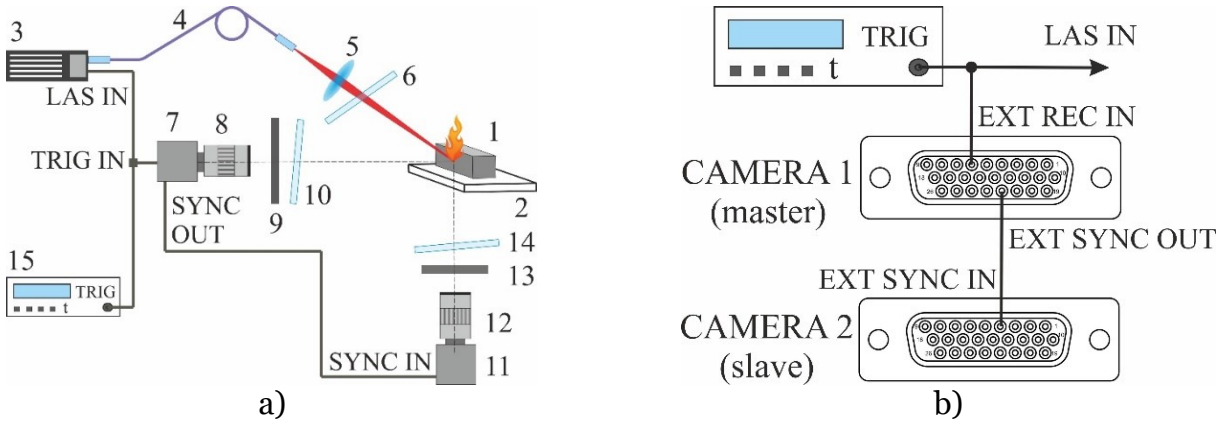

Fig. 1. Two-angle scheme of direct visualization (a) and connection diagram of high-speed camera connectors (b). 1 – sample; 2 – substrate; 3 – initiating laser; 4 – fiber optic light guide; 5 – lens; 6, 10, 14 – protective glass; 7 – front camera (camera 1); 8, 12 – objective lenses; 9, 13 – gray filters; 11 – side camera (camera 2); 15 – pulse generator.

During recording, the master camera generates “EXT SYNC OUT” pulses with a duration of 3.2 μs, synchronous with the camera exposure. To synchronize two cameras, pulses from the “EXT SYNC OUT” output of the master camera are fed to the “EXT SYNC IN” input of the slave camera (Fig. 1b). The slave camera mode is set in the service program. A feature of the Evercam 1000-16-S camera in slave mode is insensitivity to the signal at the “EXT REC IN" input. Image recording is determined only by the presence of sync pulses at the "EXT SYNC IN” input. At the same time, the slave camera also generates “EXT SYNC OUT” pulses, from which we can conclude that the cameras are working synchronously. Fig. 2 shows the oscillograms of the synchronization pulses.

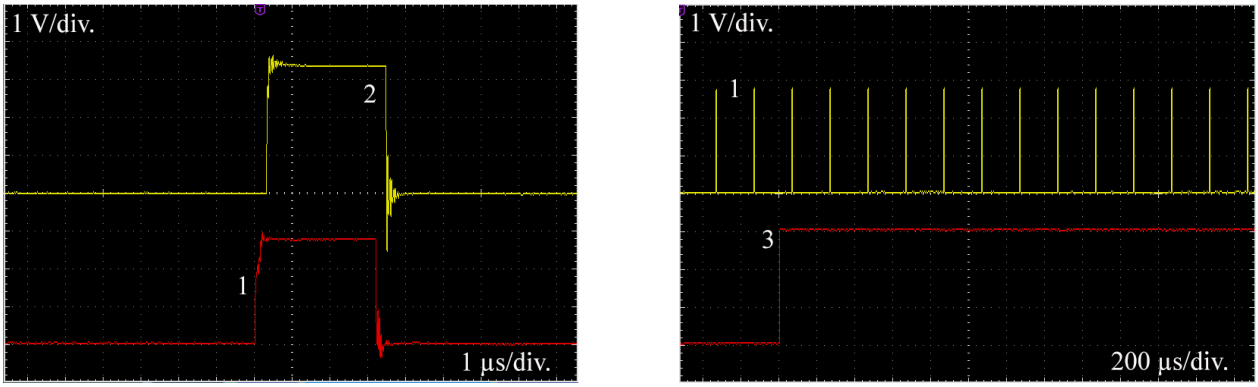

a) b)

Fig. 2. Oscillograms of synchronization pulses. a – sync pulses “EXT SYNC OUT” of the master (1) and “EXT SYNC OUT” slave (2) cameras; b – synchronization pulses “EXT SYNC OUT” of the master camera (1) and laser radiation resolution pulse/“EXT REC IN” (3).

The delay between the “EXT SYNC OUT” pulses of the cameras is 0.3 μs, the delay relative to the “EXT REC IN” signal is 60 μs. An SDS70102V oscilloscope was used to record the waveforms. Thus, the beginning of exposure to the initiating laser and the start of shooting of both cameras occur almost simultaneously. This makes it possible to study the process of laser initiation, starting from the first moments of the heating action of the laser.

2.3 Laser monitor

Fig. 3 depicts a scheme of a laser monitor with two Evercam 1000-16-C cameras. The design of the optical part of a laser monitor is similar to that used in [19]. The image is formed by a 10 cm diameter lens *18* with a focal length of 50 cm. The diameter of the area illuminated by the brightness amplifier is 4.5 mm. The output radiation of the brightness amplifier is focused on the matrix of the high-speed camera *7* with the lens *8* MC Zenitar 1.2/50s. The recorded observation area is 4.0×1.2 mm² with a spatial resolution of 12.5 microns. The spread of combustion products during the combustion of the Al-CuO thermite mixture can exceed 50 cm, therefore, a protective quartz glass is installed in front of the lens.

We used a copper bromide vapor brightness amplifier based on the gas discharge tube (GDT) with a diameter of 3 cm and a length of the active part (inside the external heater) of 60 cm. The GDT had a sealed-off construction with external heating of the gain medium, similar to that previously used in systems with brightness amplification in [6, 7, 20]. The design features of the GDT are given in [20]. A power supply with a pulsed charge of the storage capacitor, considered in [20], was used to pump the active medium. The pulse repetition frequency (PRF) of the pumping source, and, consequently, the PRF of the laser radiation, was 20 kHz. The operating conditions were optimized to ensure a uniform beam profile of enhanced spontaneous emission (ASE) and a relatively low average power of ASE – 26 mW at a wavelength of 510.6 nm. This mode of operation of the brightness amplifier is considered in [27]. The low average ASE power with a relatively large observation area provided an extremely low power density of the laser monitor radiation on the surface of the object of study

(1.6 mW/mm²), had no noticeable effect on the surface of the object of visualization and excluded the possibility of uncontrolled initiation.

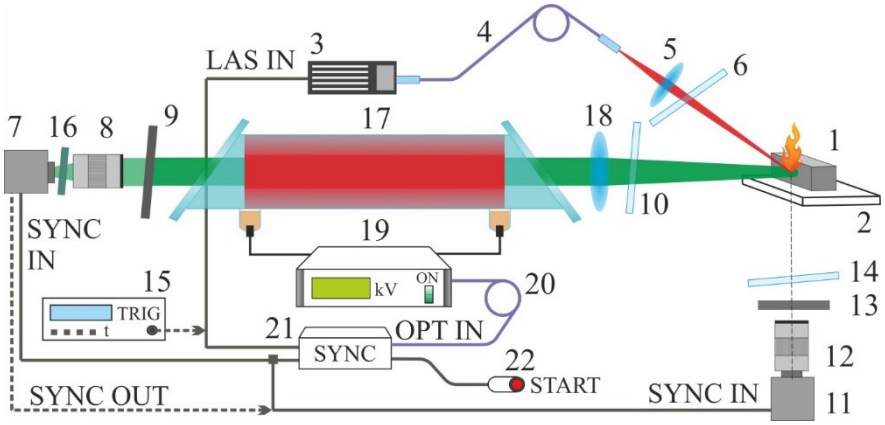

Fig. 3. Laser monitor. 1 – sample; 2 – substrate; 3 – initiating laser; 4 – fiber optic light guide; 5 – lens; 6, 10, 14 – protective quartz plates; 7 – laser monitor camera; 8, 12 – lenses; 9, 13 – gray filters; 11 – side camera; 15 – external generator; 16 – 510±5 nm filter; 17 – brightness amplifier; 18 – image-forming lens; 19 – power supply for a brightness amplifier; 20 – fiber optic light guide; 21 – synchronization unit; 22 – start button.

Despite the high brightness of the radiation on the green line of the brightness amplifier (510.6 nm), installing only a gray filter *9* between the brightness amplifier and the lens *8* was not enough to suppress the illumination created by the brightness glow of the object of study passing along the optical path of the laser monitor. The thermite mixture Al-CuO combustion is currently the most brightly glowing object studied using a laser monitor. In this regard, it was necessary to install a bandpass filter *16* with a bandwidth of 510±5 nm.

The side-mounted high-speed camera Evercam 1000-16-C *11* with a lens MC Zenitar 1.2/50s *12* was installed at an angle of 90° to the optical axis of the brightness amplifier. Gray filters of the HS type were installed in front of the lens to reduce the illumination. Image recording, as in the two-angle scheme, was carried out at a speed of 5000 frames/s; the spatial resolution of the matrix was set at 640×192 pixels for both side images in their own glow and for images of the laser monitor.

The brightness amplifier operates in a pulsed high-frequency mode with a pulse duration of tens of nanoseconds [20, 21]. Thus, in order to ensure the same exposure of the high-speed camera matrix, it is necessary to synchronize the sequence of shooting frames with the sequence of radiation pulses of the active medium of the brightness amplifier. The camera matrix can be exposed by one or several pulses of laser radiation [19].

In this work, synchronization is performed using the STM32F103C8T6 microcontroller board. The view and pin scheme of the synchronization unit is shown in Fig. 4.

To minimize interference from high-voltage pulses of the power supply, the electronic circuit is placed in a metal case, and the input and output signals are optically isolated. Via the optical fiber channel “OPT IN” (20 in Fig. 3), implemented using the HFBR-0500Z kit, pulses synchronous with the active medium pumping pulses are fed to the input of the microcontroller. The inputs of the microcontroller also receive signals from the “START” button or from an external pulse generator “TRIG”.

a)

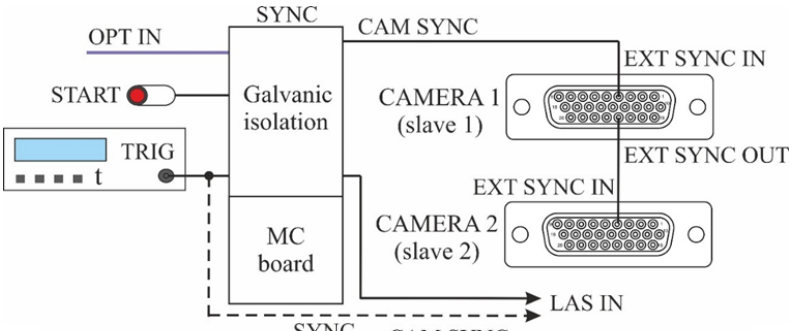

b)

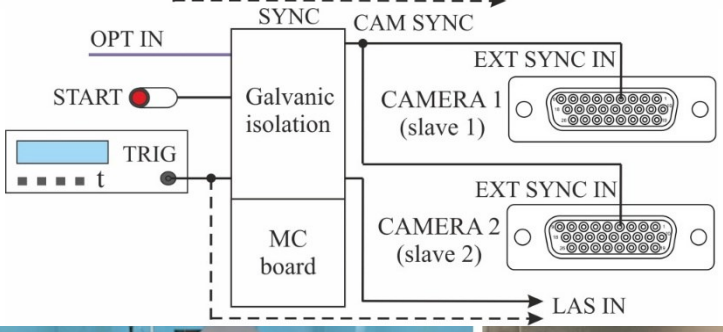

c)

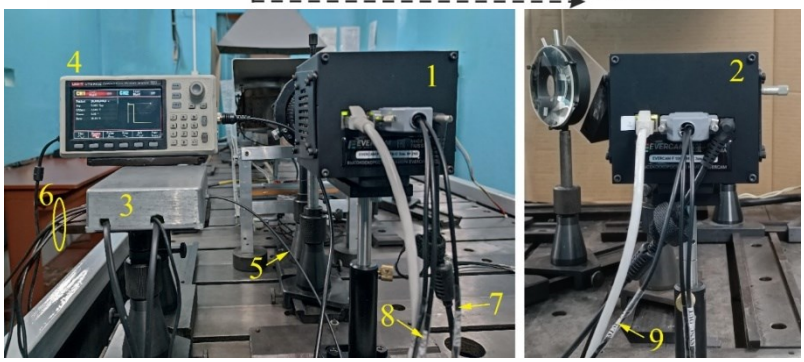

Fig. 4. Synchronization scheme based on the STM32F103C8T6 microcontroller board. a – serial synchronization; b – parallel synchronization; c – photo of the synchronization unit and connection of high-speed cameras. 1 – slave camera 1 (as part of a laser monitor); 2 – slave camera 2 (side camera); 3 – synchronization unit; 4 – external generator; 5 – optical channel "OPT IN"; 6 – outputs and inputs of the synchronization unit; 7 – "EXT SYNC IN" input of the slave camera 1; 8 – output "EXT SYNC OUT" of the slave camera 1; 9 – input "EXT SYNC IN" of the slave camera 2.

The microcontroller generates two output signals: the external synchronization signal "CAM SYNC" for the high-speed camera and the enable signal "LAS IN" for the initiating laser (Fig. 5). The input and output signals of the microcontroller are galvanically isolated using FOD817 optocouplers. The synchronization unit has two galvanically isolated power supplies.

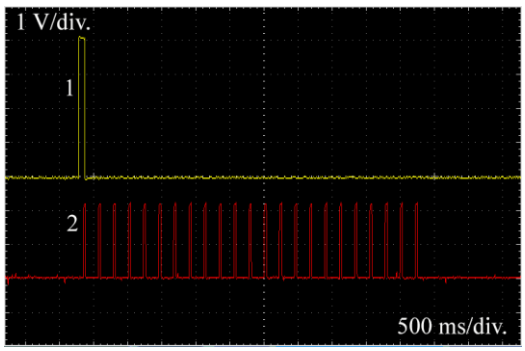

a)

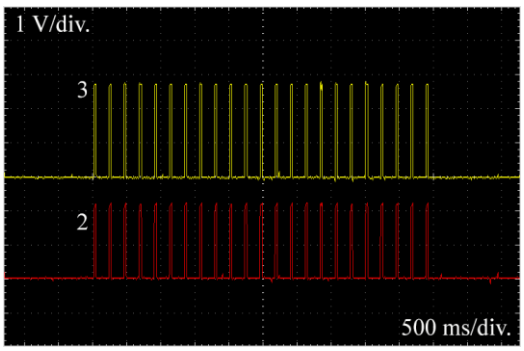

b)

Fig. 5. Oscillograms of synchronization pulses. a – lasing enabling pulse LAS IN (1) and CAM SYNC signal (2) of the synchronization unit; b – EXT SYNC IN/CAM SYNC (2) and EXT SYNC OUT (3) sync pulses of the master camera 1.

The microcontroller program has five preset values for the duration of the initiating laser pulse, selected by the switch, to affect the test sample for the operation mode started by the “START” button. After pressing this button, a “LAS IN” signal and a train of “CAM SYNC” pulses are generated, which is illustrated by the waveforms in Fig. 5.

The number of pulses in the train is preset by the microcontroller program. It is important to ensure that this value is less than the value set in the service program to avoid overwriting frames and loss of the initial recording fragment. If the pulse duration of the initiating laser is required, which differs from the preset ones, an external generator is used. The signal from the external generator is fed directly to the laser enabling input; the generating of the “CAM SYNC” pulse train also begins with this signal. Since the recording start time is arbitrary with respect to the emission pulses of the brightness amplifier, the delay of the first “CAM SYNC” pulse with respect to the front of the “LAS IN” signal varies from 200 to 250 μs.

There are five preset values in the microcontroller program (4, 6, 10, 20, 40) for the frequency division coefficient of the pulses coming through the optical channel from the power supply of the brightness amplifier. Thus, the synchronization unit generates trains of pulses with frequencies of 5.0, 3.33, 2.0, 1.0 or 0.5 kHz synchronized with the emission pulses of the brightness amplifier. The pulses of these trains serve as synchro pulses for recording frames by digital cameras at recording speeds of 5000, 3333, 2000, 1000 and 500 frames/sec, respectively.

We have tested two options for synchronizing shooting with two Evercam 1000-16-C cameras. For both cameras, the "slave" mode was set in the service program. Which of the cameras in the laser monitor *7* or the side *11* in Fig. 3 is slave 1 or slave 2 does not matter. In the first synchronization variant, pulses from the “EXT SYNC OUT” output of the slave camera 1 were fed to the “EXT SYNC IN” input of the slave camera 2 (Fig. 4a). At the same time, “CAM SYNC” pulses from the synchronization unit were applied to the “EXT SYNC IN” input of the slave camera 1. It is important to note that the duration of the “EXT SYNC OUT” signal of the slave camera 1, as well as the slave camera 2, repeats the duration of the signal at the “EXT SYNC IN” input (40 μs).

In the second variant, “CAM SYNC” pulses from the synchronization unit were fed to the “EXT SYNC IN” inputs of both cameras. Accordingly, the “EXT SYNC OUT” output was not connected. Since the delay in generating the “EXT SYNC OUT” signal in relation to “EXT SYNC IN” is 0.3 microseconds, it is not critical. Therefore, both synchronization modes are acceptable and provide the required shooting mode.

3. Application of visualization schemes

3.1 Two-angle visualization of combustion

Fig. 6 presents the results of visualization of the combustion process of the Al-CuO sample obtained using a two-angle visualization scheme. Obviously, the area of laser exposure is better visible in the images of the front camera, which makes it possible to record the dynamics of the process, starting from the first moments of the heating action of the initiating laser. According to the data of this camera, the time of the combustion of the sample (110.6 ms) was determined. This parameter is important for estimating the initiation energy.

Based on two sequences of images of the process, it is possible to analyze the combustion dynamics – changes in the flame propagation velocity during the process. The distance to which the flame front has shifted is determined from the frames of the high-speed recording. The time is calculated based on the number of frames corresponding to this distance. The flame propagation velocity is determined by distance and time. The calculation results are shown in Fig. 7.

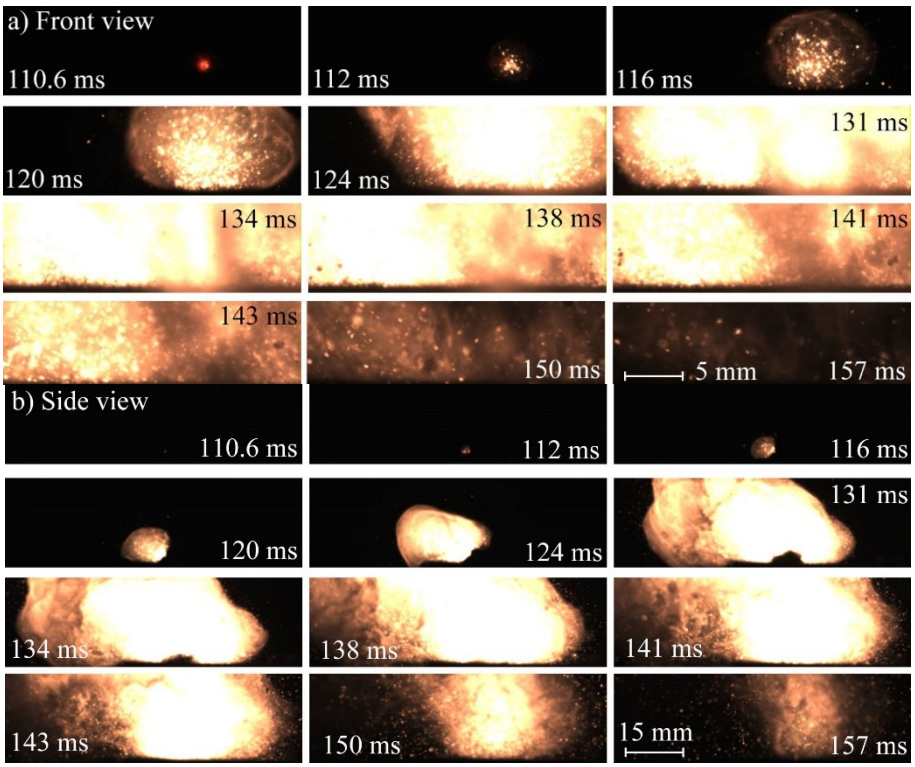

Fig. 6. Visualization of the combustion of the Al-CuO mixture (sample 1) in the two-angle scheme (Fig. 1a). a – front view; b – side view.

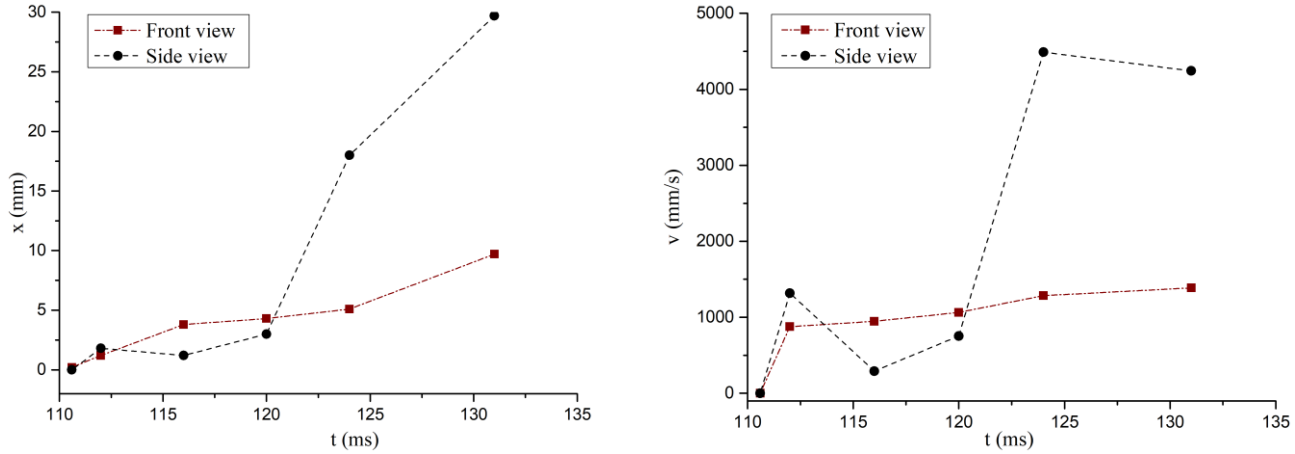

a) b)

Fig. 7. The displacement (a) and the propagation velocity of the combustion front (b) corresponding to the process in Fig. 6

It follows from the data obtained that the flame propagation velocity in the horizontal and vertical directions may differ within the order of magnitude. The data obtained can be used to develop or verify a spatial model of the combustion of the Al-CuO thermite mixture.

3.2 Visualization using a laser monitor

The difference between laser monitoring and direct high-speed imaging is the observation of the surface over which the combustion spreads. Fig. 8 shows frames of high-speed video recording of laser monitor images, synchronized with frames of direct video shooting from the side.

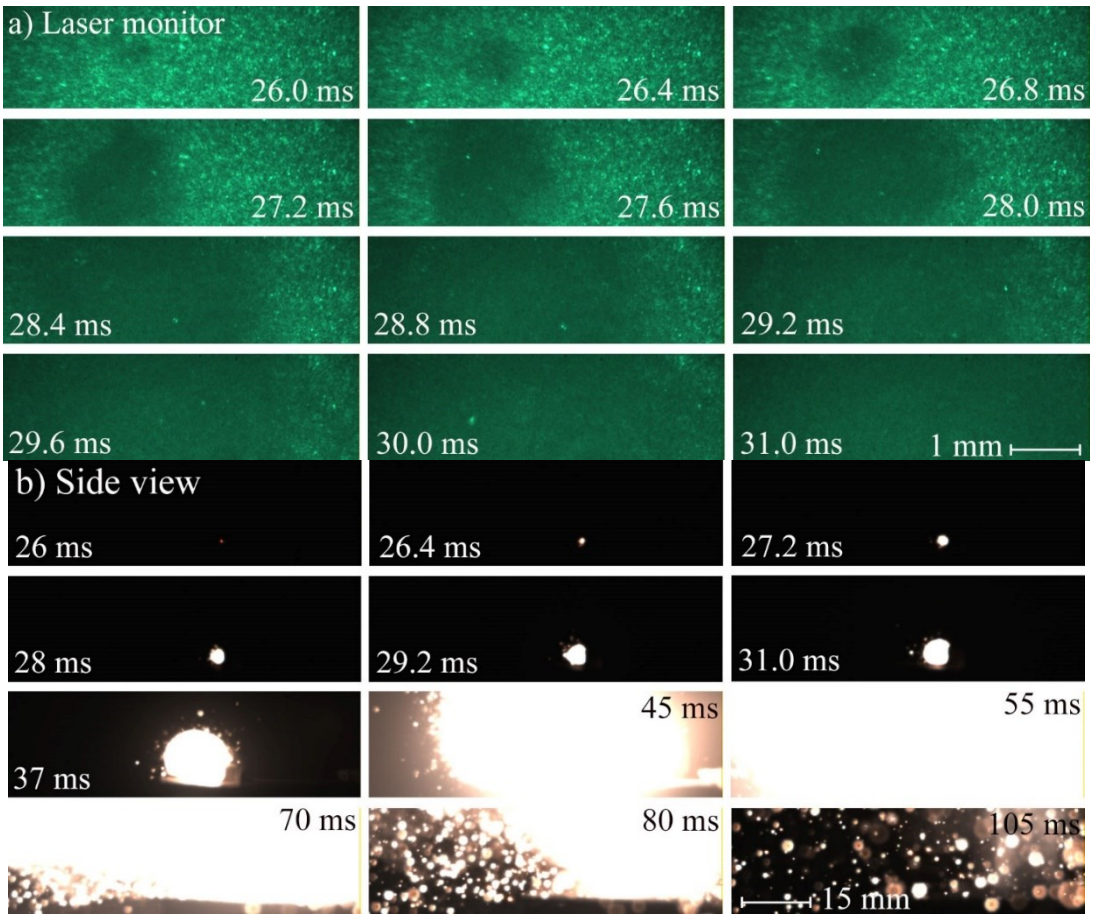

Fig. 8. Visualization of combustion of the Al-CuO mixture (sample 2) in the laser monitor scheme (Fig. 3). a – image of the laser monitor; b – side view

The process time calculated from the images of the laser monitor represents the time of the process in the field of view only. The side camera provides an overview of the entire combustion process. Fig. 9 shows graphs of the change in the velocity of propagation of the combustion front over the surface and the corresponding flame propagation. The data demonstrate a significant inhomogeneity of the combustion of the studied mixture.

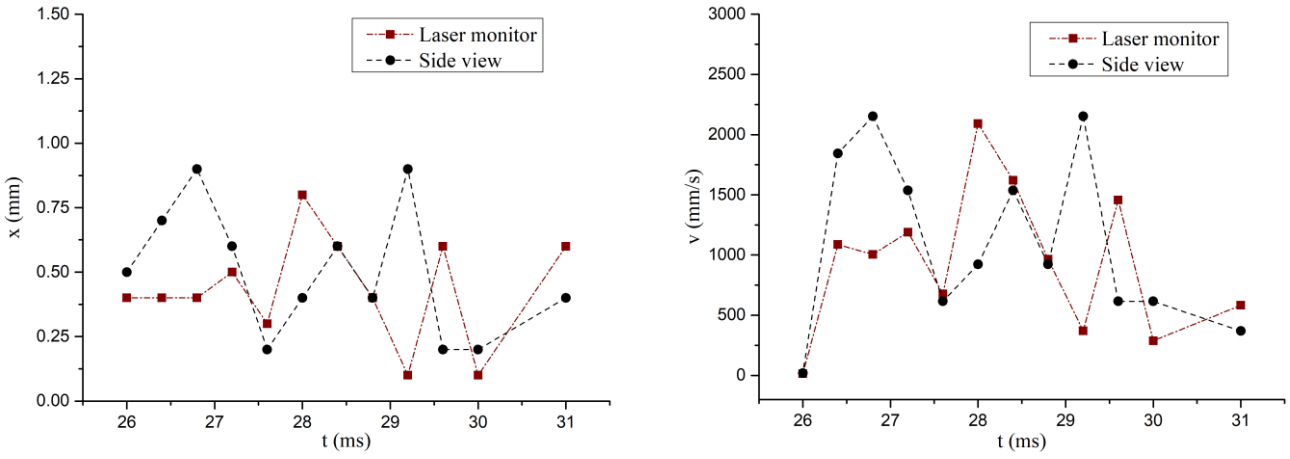

Fig. 9. The displacement (a) and the velocity of propagation of the combustion front (b) corresponding to the process in Fig. 8

4. Conclusion

The paper considers the synchronous operation of two high-speed cameras Evercam F 1000-16-C (Russia) as part of a two-angle high-speed visualization scheme and for recording images in a visualization scheme with brightness amplification (laser monitor). To implement the operation of the Evercam F 1000-16-C high-speed camera as part of a laser monitor with a copper bromide brightness amplifier, a synchronization circuit based on the STM32F103C8T6 microcontroller board has been developed. The circuit allows us to implement a train image recording mode.

For the first time, these cameras were used for high-speed visualization of laser initiation and high-temperature combustion of thermite mixture with a burning rate of up to 4.5 m/s (Al-CuO nanopowders mixture). In the two-angle visualization scheme, the flow of the combustion process of the sample is synchronously recorded from two positions, which makes it possible to determine not only the temporal characteristics of the process in different directions, but also to form a spatial representation of the parameters and intensity of the radiation accompanying combustion. Thus, it is possible to obtain data for developing or verifying a 3D model of combustion process.

The experience gained using Evercam F 1000-16-C cameras and the implementation of a laser monitor using these cameras will be used in the future for a more detailed study of the combustion of thermite mixtures and other high-energy materials.

Acknowledgements

The authors express their gratitude to the staff of the Laboratory of Physicochemistry of Highly Dispersed Materials of the Institute of Strength Physics and Materials Science SB RAS (Tomsk) for the nanopowders provided.

The preparation of nanopowder mixtures was carried out using the equipment of the Center for Advanced Materials and Technologies of Sevastopol State University.

References

1. Znamenskaya I.A., Karnozova E.A., Muratov M.I., Lutsky A.E. Thermographic visualization in high speed gas dynamic flows // Proceedings of the XVII International Scientific and Technical Conference. Moscow: Scientific and Technological Center of Unique Instrumentation of the Russian Academy of Sciences, 2023. – pp. 138-146 [in Russian].

2. Sergeev D.A., Troitskaya Yu.I., Cherdantsev A.V. Investigation of the spray generation due to bag breakup fragmentation phenomena with optical methods in environmental and technical systems // Scientific Visualization, Vol. 15, № 3, 2023, (doi: 10.26583/sv.15.3.09) (https://sv-journal.org/2023-3/09/).

3. Trigub M.V., Malakhov D.V., Stepakhin V.D., Evtushenko G.S., Balabanov D.A., Skvortsova N.N. High-speed imaging of plasmachemical synthesis in fast-flowing chain processes initiated by gyrotron radiation // Atmospheric and Oceanic Optics, Vol. 33, № 3, 2020, pp. 199-204 (doi: 10.15372/AOO20200308) [in Russian].

4. Bolotov S.V., Homchenko A.V., Shul'ga A.V., Bolotova E.L. Information-measuring complex for investigation of melting and electrode metal transfer of arc welding // Bulletin of the Bryansk State Technical University, Vol. 91, №6(91), 2020, pp. 4-11 [in Russian].

5. Dyachkov Yu.A., Krasnov M.N.., Kamshin S.V., Novichok S.A., Korotkov D.I. Experimental study of a full-scale model of a muzzle brake of a small caliber // Voennoe obozrenie [Military Review], №2(12), 2022, pp.30-34 [in Russian].

6. Gubarev F.A., Kim S., Li L., Mostovshchikov A.V., Il'in A.P. High-speed optical imaging technique for combusting metal nanopowders // Instruments and Experimental Techniques, №63(3), 2020, pp. 375-382 (doi: 10.1016/j.optlastec.2022.108981)

7. Li L., Mostovshchikov A.V., Ilyin A.P., Antipov P.A., Shiyanov D.V., Gubarev F.A. In situ nanopowder combustion visualization using laser systems with brightness amplification

// Proceedings of the Combustion Institute, Vol. 38, 2021, pp. 1695–1702 (doi: 10.1016/j.proci.2020.08.048)

8. Jiang Y., Wang Y., Baek J., Wang H., Gottfried J.L., Wu C.-C., Shi X., Zachariah M.R., Zheng X. Ignition and combustion of Perfluoroalkyl-functionalized aluminum nanoparticles and nanothermite // Combustion and Flame, Vol. 242, 2022, 112170 (https://doi.org/10.1016/j.combustflame.2022.112170)

9. Wainwright E.R., Dean S.W., Vummidi Lakshman S., Weihs T.P., Gottfried J.L. Evaluating compositional effects on the laser-induced combustion and shock velocities of Al/Zr-based composite fuels // Combustion and Flame, Vol. 213, 2020, pp. 357-368 (https://doi.org/10.1016/j.combustflame.2019.12.009)

10. Kline D.J., Alibay Z., Rehwoldt M.C., Idrogo-Lam A., Hamilton S.G., Biswas P., Xu F., Zachariah M.R. Experimental observation of the heat transfer mechanisms that drive propagation in additively manufactured energetic materials // Combustion and Flame, Vol. 215, 2020, pp. 417-424, (https://doi.org/10.1016/j.combustflame.2020.01.020)

11. Dolgoborodov A.Yu, Kirilenko V.G., Brazhnikov M.A., Grishin L.I., Kuskov M.L., Valyano G.E. Ignition of nanothermites by a laser diode pulse // Defence Technology, Vol. 18, I. 18, 2022, pp. 194-204 (doi: 10.1016/j.dt.2021.01.006)

12. Gromov A.A., Khabas T.A., Ilyin A.P., Popenko E.M., Korotkov A.G., Arkhipov V.A., Dietz A.A., Strokova Yu.I., Tolbanova L.O. Gorenie nanoporoshkov metallov [Metal nanopowders combustion]. Tomsk: Deltaplan, 2008 [in Russian].

13. Manin J., Skeen S.A., Pickett L.M. Performance comparison of state-of-the-art high-speed video cameras for scientific applications // Optical Engineering, Vol 57, I. 12, 2018, 124105 (doi: 10.1117/1.OE.57.12.124105)

14. Li L., Ilyin A.P., Gubarev F.A., Mostovshchikov A.V., Klenovskii M.S., Study of self-propagating high-temperature synthesis of aluminium nitride using a laser monitor // Ceramics International, Vol. 44, № 16, 2018, (doi:10.1016/j.ceramint.2018.07.237)

15. Zepper E.T., Pantoya M.L., Bhattacharya S., Marston J.O., Neuber A.A., Heaps R.J. Peering through the flames: imaging techniques for reacting aluminum powders // Applied Optics, Vol. 56, 2017, pp. 2535-2541 (doi:10.1364/AO.56.002535)

16. Wang H., Kline D.J., Biswas P., Zachariah M.R. Connecting agglomeration and burn rate in a thermite reaction: Role of oxidizer morphology // Combustion and Flame, Vol. 231, 2021, 111492, (https://doi.org/10.1016/j.combustflame.2021.111492)

17. Baranov P.S., Mantsvetov A.A., Belous D.A., Dmitrieva A.U. The designing of the television systems for registration high-rate processes // Voprosy radioelectroniki. Seriya: Tehnika televideniya [Questions of radio electronics. Series: Television technology], №4, 2017, pp. 35-43 [in Russian].

18. Vision Research Inc. https://www.phantomhighspeed.com/products (Access date: 04/07/2024)

19. Gubarev F.A., Mostovshchikov A.V., Li L. Two-brightness-amplifier imaging system for energetic-materials-combustion study // Optics and Laser Technology, Vol. 159, 2023, 108981 (doi:10.1016/j.optlastec.2022.108981)

20. Burkin E.Y., Gubarev F.A., Sviridov V.V., Shiyanov D.V. Two-channel power supply for an imaging system with copper bromide vapor brightness amplifiers // Iranian Journal of Electrical and Electronic Engineering, Vol. 19, № 3, 2023 (https://doi.org/10.22068/IJEEE.19.3.2617)

21. Petrash G.G. Opticheskie sistemy s usilitelyami yarkosti [Optical systems with brightness amplifiers]. M.: Nauka, 1991 [in Russian].

22. Evtushenko G.S. Methods and instruments for visual and optical diagnostics of objects and fast processes. Nova Science Publishers. New York, USA, 2018.

23. High-speed cameras EVERCAM, EVERCAM F, EVERCAM HR, EVERCAM HS, EVERCAM L, EVERCAM FL. User's Guide. Version 5.00. https://evercam.ru/dokumentatsiya/ (Access date: 04/07/2024)

24. Pervikov A., Toropkov N., Kazantsev S., Bakina O.V., Glazkova E., Lerner M. Preparation of nano/micro bimodal aluminum powder by electrical explosion of wires // Materials, № 21, 2021 (doi:10.3390/ma14216602)

25. Toropkov, N.E., Sagun, A.I., Kudryashova, O.B., Lerner, M.I. Optimal Conditions for ultrasonic treatment of powder suspensions to obtain homogeneous thermite mixtures // Russian Physics Journal, Vol. 66, № 9, 2023, pp. 978-982 (doi: 10.1007/s11182-023-03032-w)

26. Petrovsky G.T. Czvetnoe opticheskoe steklo i osoby`e stekla [Color optical glass and special glasses]. M.: Dom Optiki, 1990 [in Russian].

27. Li L., Shiyanov D.V., Gubarev F.A. Spatial–temporal radiation distribution in a CuBr vapor brightness amplifier in a real laser monitor scheme // Applied Physics B: Lasers and Optics, Vol. 126, № 10, 2020, 155 (https://link.springer.com/article/10.1007/s00340-020-07511-7)